Forsch Ingenieurwes (2011) 75:183–196
DOI 10.1007/s10010-011-0144-5

ORIGINALARBEITEN/ORIGINALS

Robust identification of pneumatic servo actuators in the real situations

V. Filipovic · N. Nedic · V. Stojanovic

Received: 26 June 2011 / Published online: 3 November 2011

Abstract Intensive research in the field of mathematical modelling of the pneumatic cylinder has shown that its mathematical model is nonlinear and that a lot of important details cannot be included in the model. Selection of the model and the identification method have been conditioned by the following facts:

(a) The nonlinear model of the system can be approximated by a linear model with time-variant parameters.
(b) There is the influence of the combination of heat coefficient, unknown discharge coefficient and change of temperature on the pneumatic cylinder model. Therefore it is assumed that the parameters of the pneumatic cylinder are random (stochastic parameters).
(c) In practical conditions, observations have a non-Gaussian distribution.

Due to the abovementioned reasons, it is assumed that the pneumatic cylinder model is a linear stochastic model with variable parameters. The Masreliez-Martin filter (robust Kalman filter) was used for identification of parameters of the model. For the purpose of increasing the practical value of the filter, the following two heuristic modifications were performed:

(1) It was adopted that $T(k) = 1$ holds for the scalar transformation of residuals.
(2) Fisher information was approximated by a derivative of the Huber's function.

The proposed modifications were confirmed through intensive simulations. In order to provide persistent excitation, the autocovariance function "$1/f$" of the signal was used. The behaviour of the new approach to identification of the pneumatic cylinder is illustrated by simulations.

V. Filipovic · N. Nedic · V. Stojanovic (✉)
Faculty of Mechanical Engineering Kraljevo, Department of Energetics and Automatic Control, University of Kragujevac, Dositejeva 19, 36000 Kraljevo, Serbia
e-mail: vladostojanovic@open.telekom.rs

Robuste Identifikation von pneumatischen Servo-Aktuatoren in der realen Situationen

Zusammenfassung Intensive Forschung auf dem Gebiet der mathematischen Modellierung des pneumatischen Zylinders hat gezeigt, dass sein mathematisches Modell nichtlinear ist und dass viele wichtige Details nicht in das Modell einbezogen werden können. Die Auswahl des Modells und die Art der Identifikation werden durch folgende Tatsachen bedingt:

(a) Das nichtlineare Modell des Systems kann durch ein lineares Modell mit zeitvarianten Parametern angenähert werden.
(b) Es besteht ein Einfluss der Kombination von Wärmedurchgangs-Koeffizient, unbekanntem Durchflusskoeffizienten und Änderungen der Temperatur auf das pneumatischen Zylinder-Modell. Es wird daher angenommen, dass die Parameter des pneumatischen Zylinders zufälligen Charakters sind.
(c) Unter praktischen Bedingungen haben die Beobachtungsergebnisse eine nicht-Gaußsche Verteilung.

Aufgrund der vorgenannten Gründe wird davon ausgegangen, dass das Pneumatikzylinder Modell ein lineares, stochastisches Modell mit variablen Parametern sein muss. Der Masreliez-Martin-Filter (robust Kalman-Filter) wurde für die Identifizierung von Parametern des Modells verwendet. Zur Erhöhung des praktischen Werts des Filters, wurden die beiden folgenden heuristischen Modifikationen durchgeführt:

(1) Es wird angenommen, dass $T(k) = 1$ für das skalare Transformation der Residuen hält.
(2) Die Fisher-Information wird durch ein Derivat des Hubers Funktion approximiert.

Die vorgeschlagenen Änderungen werden durch intensive Simulationen bestätigt. Um für eine anhaltende Erregung zu sorgen, wird die Autokovarianzfunktion "$1/f$" des Signals verwendet. Das Verhalten des neuen Ansatzes zur Identifikation des pneumatischen Zylinders wird durch Simulationen aufgezeigt.

List of symbols

P_S	supply pressure
P_i	pressure in the chamber $i = a, b$
P_o	outer absolute pressure
m	total mass of the piston and the load
β_e	nonlinear viscous friction coefficient
k_e	load spring gradient
F_{ext}	load force disturbance on the piston
F_f	friction forces
A_i	effective area of the piston
T_S	supply temperature
R	the universal gas constant
$\dot{m}_l$	leakage mass flow rate between the cylinder chambers
$\dot{m}_i$	mass flow rates through the orifice $i = a, b$
$C_d(t)$	valve discharge coefficient
$\alpha(t)$	heat coefficient
$\beta(t)$	uncertain bound parameter
$\tau(t)$	variation of the temperature
W	port width
y	displacement of the piston
$y(k)$	discrete scalar observations of the piston displacement
$x(k)$	discrete time $n \times 1$ state vector
$u(k)$	input signal
$F(k)$	$n \times n$ state transition matrix
$H(k)$	$1 \times n$ observation matrix
$w(k)$	process noise
$v(k)$	measurement noise
$T(k)$	a linear transformation
$W(k)$	covariance for process noise $w(k)$
$P(k\|k-1)$	a priori covariance matrix
$P(k\|k)$	a posteriori covariance matrix
$E_{P_\varepsilon}\{\cdot\}$	expectation with respect to the least favourable pdf
$I(p)$	Fisher information for the least favourable pdf
ε	degree of contamination
$\psi_p[\cdot]$	vector influence function
$\varphi(k)$	$1 \times n$ regression vector
$\theta(k)$	$n \times 1$true parameter vector
$\bar{\theta}$	mean value of true parameter vector
Σ_θ	covariance matrix of true parameter vector
$\hat{\theta}(k)$	estimation of true parameter vector
C	a priori known non-singular matrix
$\hat{y}(k)$	adjustable predictor
a_i, b_j	system parameters ($i = 1, \ldots, n$; $j = 1, \ldots, m$)
$r_k^d, \hat{r}_k$	desired and non central autocovariances of excitation signal
s_t	excitation signal
$\phi^{1/f}$	spectrum of bandlimited noise
$\omega, \underline{\omega}, \bar{\omega}$	frequency and its lower and upper limits

Subscripts

a	head side of the piston
b	rod side of the piston

Abbreviations

ARX	autoregressive with exogenous input
ARMA	autoregressive moving average
ARMAX	autoregressive moving average with exogenous input
RLS	recursive least square
OE	output error
MSE	mean square error
SISO	single input/single output
pdf	probability density function

1 Introduction

Since pneumatically driven systems have a lot of distinct characteristics of energy-saving, cleanliness, simple structure and operation, and high efficiency and are suitable for working in a harsh environment, they have been extensively used for many years in robot driven systems and industrial automation [1]. However, pneumatic actuators are characterized by high-order time-variant dynamics, nonlinearities due to the compressibility of air, internal and external disturbances, and payload variations [2–4]. It is difficult to build an accurate dynamic model for describing pneumatic servo-drive behaviour. Therefore, in order to design controllers that are reliable and easy to understand in practice, simplified plant models are obtained by linearization around operating points [5–8].

The purpose of this paper is to use the theory and findings of system identification to obtain a mathematical model, so that the controller can be designed on the basis of the model. Numerous researchers have employed auto-regressive (moving average) with exogenous input AR(MA)X models and recursive algorithms in their work. Östring et al. [9] identified the behaviour of an industrial robot in order to model its mechanical flexibilities, while Johansson et al. [10] used a state-space model to identify the robot manipulator dynamics. Although, it is possible to obtain a linear model for a single-link flexible robot [11, 12], massive problems occur

when trying to obtain an accurate analytical model for multi-link flexible robots in practice, as the extent of the equations grows rapidly with each additional link. Tutunji et al. [13] used a recursive least squares (RLS) algorithm to identify gyroscopic system behaviour. Their results showed that an RLS algorithm based on ARMA models provides a reasonably accurate transfer function of the systems under study. Assuming most parameters in pneumatic servo system do not change during operation, Shih and Tseng [14] performed the identification offline and adjusted servo-control before the operation accordingly. Furthermore, they investigated the impact of different parameters (sampling time, order model, different supply pressures, etc.) in the identification process. They used RLS identification algorithm based on ARX models.

The mentioned references consider the linear models of the pneumatic cylinder which are ad hoc adopted, without considering justification of such an approach. It is necessary to notice the following details:

i. The pneumatic cylinder is a nonlinear system (presence of friction force)
ii. There is a significant influence of the combination of the heat coefficient, unknown discharge coefficient and change of temperature on the behaviour of the pneumatic cylinder [15]. The mentioned influences cannot be easily included in the cylinder model and have random character.

On the other hand, recent research has shown that the nonlinear model of the system can be approximated by a linear system with time-variant parameters [16]. In this paper it is assumed that the parameters of the pneumatic cylinder model change randomly. The change of parameters is described by the random walk method, where the corresponding noise is modelled as the Gaussian stochastic process. The output error (OE) method is used as the identification algorithm. It is assumed that the measurement noise is non-Gaussian. Justification of this approach was confirmed in practice [17]. Namely, in measurements there are rare, inconsistent observations with the largest part of population of observations (outliers). Their presence can considerably degrade the performance of linearly recursive algorithms based on the assumptions that measurements have a Gaussian distribution. Therefore, synthesis of robust algorithms is of primary interest. The synthesis is based on Huber's theory of robust statistics [18]. Robustness of algorithms is accomplished by introducing the nonlinear transformation of prediction error (Huber's function).

The Masreliez-Martin filter (robust Kalman filter) is the natural frame for realization of the described algorithm. The model in the state space in which the process noise has a Gaussian distribution, and the measurement noise has a non-Gaussian distribution corresponds to the adopted model for the pneumatic cylinder.

In order to increase flexibiilty, in terms of practical application of the robust Kalman filter, the following two heuristic modifications were performed:

i. The scaling factor was adopted to be $T(k) = 1$
ii. The Fisher information in the a posteriori covariance matrix of the filter was approximated by a derivative of Huber's function.

The heuristic modifications were confirmed by intensive simulations. The side benefit obtained by intervention (ii) is the increase in the rate of convergence of estimated parameters. The reason is the increase in the robust Kalman filter gain.

The paper also considers the possibility of synthesis of the input signal in the system identification phase (experiment design), which increases the rate of convergence of estimated parameters. Experiment design is based on the theory of predictive regulators whose input signal belongs to the finite alphabet.

The illustration of behaviour of the proposed algorithm is presented through simulations.

2 Modelling of the pneumatic servo-system

This section is devoted to derivation of a mathematical model for the pneumatic servo-system and includes the most relevant dynamic and nonlinear effects that are involved in pneumatic servo-systems. The system under consideration consists of an electro-pneumatic position control servo drive and a pneumatic actuator with a load as shown in Fig. 1. The external load consists of the mass of external mechanical elements connected to the piston and a force produced by an environmental interaction.

The present model was established considering the following assumptions:

- the air flow media is a perfect gas,
- the air chamber's thermodynamic states (pressure, temperature and density) within the system components are homogenous,
- the entire system's air temperature varies from its nominal value,
- the servovalve is characterized by one uncertain discharge coefficient,
- the motion of the (piston+rod+load) may be assembly conducted under friction,
- the process is polytrophic,
- the servovalve dynamics are negligible.

2.1 Force balance equation for the piston

Applying Newton's second law to the forces on the piston, the resulting force equation is

$$A_a P_a - A_b P_b = m\ddot{y} + \beta_e \dot{y} + F_f(\dot{y}) + k_e y + F_{ext} \qquad (1)$$

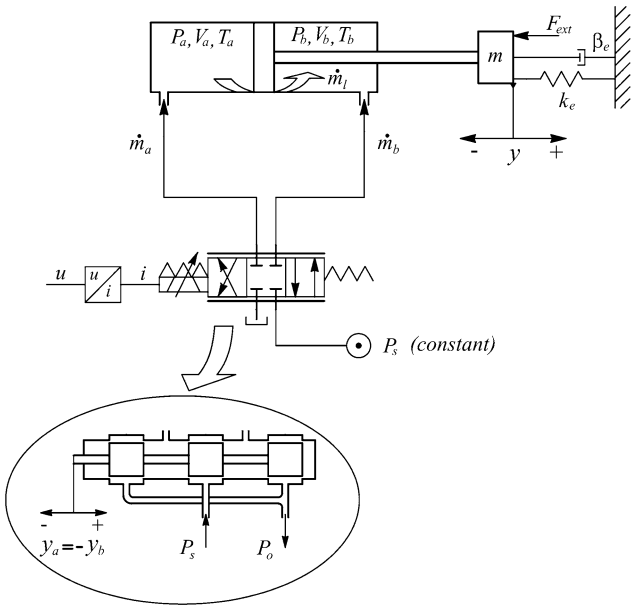

Fig. 1 Schematic representation of the valve-controlled asymmetric piston

where P_a and P_b denote the pressure of the chamber a and b, respectively, m denotes the total mass of the piston and the load referred to the piston, y is the piston displacement, β_e is the nonlinear viscous friction coefficient, k_e denotes the load spring gradient; and F_{ext} denotes the load force disturbance on the piston. The term F_f in (1) describes the summing nonlinear effects of static and Coulomb friction forces of the system. The detailed analysis for the influences of friction forces can be found in [19].

The area ratio of the asymmetric piston is $A_a/A_b > 1$, where A_a is the effective area of the head side of the piston, and A_b is the effective area of the rod side of the piston, see Fig. 1.

2.2 Pressure dynamics in the cylinder chambers

The governing equations of the pneumatic cylinder dynamic behaviour rely entirely on the study of charging and discharging processes of air to the controlled volume in the cylinder chambers. The traditional approach to the analysis is based on linearization, which makes the analysis valid only for small perturbations about an operating point [5–8]. Figure 1 illustrates schematically the relationship of the cylinder's chambers and the inlet connections. Pressure dynamics in the chambers, for $i = a, b$, is given by [15]

$$\frac{dP_i}{dt} = -\alpha(t) g_i(P_i, y, \dot{y}) + \beta(t) h_i(t, P_i, y) u_1 \tag{2}$$

in which

$$g_i(P_i, y, \dot{y}) = \frac{P_i \dot{V}_i(\dot{y})}{V_i(y)} \tag{3}$$

and

$$h_i(t, P_i, y) = \frac{\sqrt{RT_S}}{V_i(y)} W f(P_i) \operatorname{sgn}(u_1) \tag{4}$$

where R is the universal gas constant, W is a spool constant, T_S is ambient absolute temperature. If it is noted that u_1 represents the control input for the five-port control valve, then it can be written that $u_1 = y_a = -y_b$ (see Fig. 1).

Notation $f(P_i)$ is given by

$$f(P_i) = \begin{cases} \bar{f}\left(\dfrac{P_i}{P_o}\right) P_o & \text{if } P_o \geq P_i \\ -\bar{f}\left(\dfrac{P_o}{P_i}\right) P_i & \text{if } P_0 < P_i \end{cases} \tag{5}$$

where P_o represents outer absolute pressure, $\bar{f}$ denotes the reduced flow function.

Uncertain heat coefficient $\alpha(t)$ depends on the actual heat transfer occurring during the process. As it can be seen from [15], $\alpha(t)$ takes values between 1 and 1.3997.

Uncertain bound parameter $\beta(t)$, which takes values between 0.075 and 1.3297 (see [15]), is used to characterize the combination of the heat coefficient $\alpha(t)$, the unknown valve discharge coefficient $C_d(t)$ and the variation of the temperature $\tau(t)$. Thus, $\beta(t)$ is generally expressed by

$$\beta(t) = \alpha(t) C_d(t) \sqrt{\tau(t)} \tag{6}$$

If the state variables and the input variables are defined as $x_1 = y$, $x_2 = \dot{y}$, $x_3 = P_a$, $x_4 = P_b$, $u_1 = y_a = -y_b$ (valve input), $u_2 = F_{ext}$ (external disturbance) then a completely nonlinear model of the pneumatic servo-system, can be written as

$$\begin{aligned} \dot{x}_1 &= x_2 \\ \dot{x}_2 &= \frac{1}{m}\left(A_a x_3 - A_b x_4 - \beta_e x_2 - F_f(x_2) - k_e x_1 - u_2\right) \\ \dot{x}_3 &= -\alpha(t) g(x_1, x_2, x_3) + \beta(t) h(t, x_1, x_3) \\ \dot{x}_4 &= -\alpha(t) g(x_1, x_2, x_4) + \beta(t) h(t, x_1, x_4) \end{aligned} \tag{7}$$

Since uncertain heat coefficient $\alpha(t)$ and uncertain bound parameter $\beta(t)$, are only known in the certain range, it can be considered that their changes have random character. Since mentioned uncertain coefficients are involved (directly or indirectly) in the state variables, previous analysis has justified the assumption that the system is considered as stochastic.

In general, the problem with complex nonlinear models, such as the pneumatic servo cylinder, is that it is difficult to choose the large number of physical parameters involved in the model. Although a lot of parameter values are known a priori with reasonable accuracy, a large number of parameters are only known within a certain range, and some are

even completely unknown. This may be due to manufacturing tolerances, or due to the fact that manufacturers do not provide parameter values because they consider them as proprietary information.

Furthermore, it is extremely difficult to accurately acquire the system parameters, such as component dimensions, internal leakage coefficients, valve discharge coefficient, spool viscous friction coefficient, static and dynamic friction force between the piston and the cylinder bore and piston viscous friction coefficient because the mentioned parameters cannot be directly measured or calculated. This causes a great difficulty in system modelling and control.

The consequence of these problems is that the theoretical model is often not useful for quantitative analysis of the pneumatic servo-system behaviour. Obviously, it is not easy to accurately derive and simulate the mathematical model of a nonlinear system.

3 Identification of the pneumatic cylinder

3.1 Robust Kalman filter as the parameter estimator

The previous section shows that the mathematical model of the pneumatic cylinder in nonlinear and that it is not possible to include a large number of important details in the model. The natural way of solving this problem is to apply the identification theory. In that case the following problems arise:

i. Type of the model (linear, nonlinear, deterministic, stochastic)
ii. Nature of disturbance (uniformly constrained, stochastic)

The following three facts have conditioned the choice of the model:

(a) Recent research has shown that the nonlinear model of the system can be correctly approximated by a system with time variant parameters [16].
(b) A more detailed analysis of the pneumatic cylinder model described in the previous section shows that the combination of heat coefficient, unknown discharge coefficient and change of temperature influences the model of cylinder [15]. Those influences are random and therefore it is assumed that the parameters of the pneumatic cylinder are random.
(c) Practical and theoretical research has shown that in a stochastic model of the system there are some observations that are inconsistent with the largest part of the population (outliers) [17], and that is why the disturbance in the model (measurement noise) is non-Gaussian.

The mentioned reasons lead to the assumption that the model of the pneumatic cylinder is a stochastic linear model with time variant parameters. As far as the authors are informed, such a pneumatic cylinder model has not been considered in the literature so far.

The change of parameters of the pneumatic cylinder will be described first. It is possible to introduce different changes of parameters (jump, continual). Taking into account the physics of the problem, it will be assumed that the change of the parameters has the form of random walk

$$\theta(k+1) = \theta(k) + w(k) \tag{8}$$

where the stochastic process $w(k)$ is Gaussian with the mean value zero and the covariance matrix $W(k)$. In this paper the Gaussian (normal) distribution will further on be denoted as $N(\bar{s}, S)$ where $\bar{s}$ is the mean value, and S is the covariance matrix.

Remark 1 It is possible to present the model (8) in a more general form

$$\theta(k+1) = C\theta(k) + w(k) \tag{9}$$

where C is the a priori known non-singular matrix. This matrix is suitable for entering a priori information on the phenomenon which is being identified.

The relation (9) results in the possibility of modelling deterministically variable parameters

$$\theta(k+1) = C\theta(k) \tag{10}$$

The output error method based on systems with a reference model will be used as a model which describes the dynamics of the pneumatic cylinder.

The output of the model without disturbance will be denoted as $y_n(k)$. The dynamics of the model in that case is described as

$$\begin{aligned} y_n(k) = &- a_1(k)y_n(k-1) - \cdots - a_n(k)y_n(k-n) \\ &+ b_1(k)u(k-1) + \cdots + b_m(k)u(k-m) \end{aligned} \tag{11}$$

Let us introduce the following vectors

$$\theta(k) = [a_1(k), \ldots, a_n(k), b_1(k), \ldots, b_m(k)]^T \tag{12}$$

$$\begin{aligned} \varphi_0(k) = &[-y_n(k-1), \ldots, -y_n(k-n), \\ &u(k-1), \ldots, u(k-m)]^T \end{aligned} \tag{13}$$

In that case the dynamics of the system with disturbance is given by the following relation

$$y(k) = \theta^T(k)\varphi_0(k) + v(k) \tag{14}$$

The disturbance $\nu(k)$ is non-Gaussian and includes the presence of outliers. Those are approximately normal distribution classes.

$$P_\varepsilon = \{p(\nu) : p(\nu) = (1-\varepsilon)p_N(\nu) + \varepsilon q(\nu)\} \tag{15}$$

where $p(\cdot)$ denotes the probability density. The probability density $p(\nu)$ represents a mixture of normal (Gaussian) distribution

$$p_N(\nu) \sim \mathrm{N}(0, \sigma_N^2) \tag{16}$$

where σ_N^2 denotes dispersion and arbitrary probability densities $q(\nu)$. The parameter $0 \le \varepsilon < 1$ is called the degree of contamination. If $\varepsilon = 0$, then the value ν has normal distribution. If $\varepsilon = 1$, then there is complete absence of the information on the probability density.

Remark 2 In applications, the class of distribution P_ε has the form

$$P_\varepsilon = \{p(\nu) : p(\nu) = (1-\varepsilon)p_N(\nu) + \varepsilon q_{N1}(\nu)\} \tag{17}$$

where $p_N(\nu) \sim N(0, \sigma_N^2), q_{N1}(\nu) \sim N(0, \sigma_{N1}^2), \sigma_{N1}^2 \gg \sigma_N^2$.

The problem with the relation (13) is that the values $y_n(k-i)$, $(i = 1, 2, \ldots, n)$ cannot be measured. Therefore, these values are calculated by using the current estimates of the parameters θ. It results in

$$\begin{aligned}\hat{y}_n(k) = {} & -\hat{a}_1(k)\hat{y}_n(k-1) - \cdots - \hat{a}_n(k)\hat{y}_n(k-n) \\ & + \hat{b}_1(k)u(k-1) + \cdots + \hat{b}_m(k)u(k-m)\end{aligned} \tag{18}$$

If the following vectors are introduced

$$\hat{\theta}(k) = [\hat{a}_1(k), \ldots, \hat{a}_n(k), \hat{b}_1(k), \ldots, \hat{b}_m(k)]^T \tag{19}$$

$$\begin{aligned}\varphi(k) = {} & [-\hat{y}_n(k-1), \ldots, -\hat{y}_n(k-n), \\ & u(k-1), \ldots, u(k-m)]^T\end{aligned} \tag{20}$$

the relation

$$\hat{y}_n(k) = \hat{\theta}^T(k)\varphi(k) \tag{21}$$

is obtained. At the moment k, before the estimate $\hat{\theta}(k)$ is known, the prediction of the model is [20]

$$\hat{y}(k) = \hat{\theta}^T(k-1)\varphi(k). \tag{22}$$

The natural definition of the prediction error is

$$\nu(k) = y(k) - \hat{y}(k). \tag{23}$$

Depending on the adopted identification criterion, using the relations (14) and (20)–(22), different recursive identification algorithms can be obtained. Let us notice that the vector $\varphi_0(k)$ from the relation (14) is replaced with the vector $\varphi(k)$ from the relation (20), so that it could be realized by the recursive algorithm.

Let us assume that the system in the state space can be described as

$$x(k+1) = F(k)x(k) + w(k) \tag{24}$$

$$y(k) = H(k)x(k) + v(k) \tag{25}$$

where

$$\begin{aligned} &x(\cdot) \in R^n, \qquad F(\cdot) \in R^{n\times n}, \qquad w(\cdot) \in R^n \\ &y(\cdot) \in R^1, \qquad H(\cdot) \in R^{1\times n}, \qquad v(\cdot) \in R^1 \end{aligned}$$

The value $x(\cdot)$ is the state vector, $y(\cdot)$ is the system output, and $w(\cdot)$ and $e(\cdot)$ are the process noise and the measurement noise, respectively. It is assumed that the process noise is Gaussian $N(0, W(k))$, where $W(k)$ is the covariance matrix, and $\nu(\cdot)$ is the measurement noise which has non-Gaussian distribution defined by the relation (15).

In [21] Masreliez and Martin proposed the robust Kalman filter for the mentioned situation. This filter has small sensitivity to the presence of outliers in comparison with the standard Kalman filter deduced for the case when the values $w(\cdot)$ and $\nu(\cdot)$ have Gaussian distribution. The filter equations are

$$\begin{aligned}\hat{x}(k|k) = {} & F(k-1)\hat{x}(k-1|k-1) \\ & + P(k|k-1)H^T(k)T(k)\psi[\nu(k)]\end{aligned} \tag{26}$$

$$\begin{aligned}P(k|k-1) = {} & F(k-1)P(k-1|k-1)F^T(k-1) \\ & + W(k-1)\end{aligned} \tag{27}$$

$$\begin{aligned}P(k|k) = {} & P(k|k-1) - P(k|k-1)H^T(k)T^2(k)H(k) \\ & \times P(k|k-1)E_{f_0}\{\psi'(\nu(k))\}\end{aligned} \tag{28}$$

In the relation (26), $\nu(k)$ represents transformed residuals

$$\nu(k) = T(k)\big[y(k) - H(k)F(k-1)\hat{x}(k-1|k-1)\big] \tag{29}$$

As the measurement equation (25) is scalar, then $T(k)$ is also a scalar. The transformation $T(k)$ was introduced so that the innovation variable $\nu(k)$ could satisfy the conditions of symmetry of certain probability densities as well as conditions for marginal probabilities [21].

The nonlinear function $\psi(\cdot)$ for the class of ε-contaminated distributions of probabilities is Huber's function and it is obtained with the application of game theory in statistics [18]. It is defined on the basis of the least favourable distribution of probability for the given class of probability distribution.

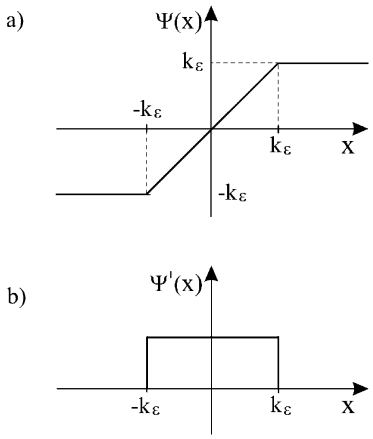

Fig. 2 Nonlinear function of residuals. (**a**) Huber's function. (**b**) Derivative of Huber's function

The originally proposed robust Kalman filter [21] (relations (26)–(28)) includes two values which are not easy to determine in practical conditions. They are the scalar transformation $T(k)$ as well as the member in the a posteriori covariance matrix $E_{f_0}\{\psi'(\nu(k))\}$. The mentioned member represents Fisher information for the least favourable probability density [22]

$$I(p)=\int_{-\infty}^{\infty}\frac{p'^2(\zeta)}{p(\zeta)}d\zeta. \tag{30}$$

In order to increase the practical values of the algorithm (26)–(28) the following heuristics were performed:

(a) For the scalar transformation $T(k)$ it has been adopted that $T(k)=1$
(b) The member $E_{P_\varepsilon}\{\psi'(\nu(k))\}$ was approximated by the realization of $\psi'(\nu(k))$.

Behaviour of the algorithms under the above modifications will be considered on the next fourth-order state estimation problem

$$x(k+1)=\begin{bmatrix}0.99 & -0.012 & 0.001 & -0.001\\ -0.005 & 0.98 & -0.001 & 0.005\\ -0.001 & 0.01 & 1 & -0.001\\ 0.01 & 0.001 & -0.002 & 1\end{bmatrix}\times x(k)+w(k) \tag{31}$$

$$y(k)=[1\quad 0\quad 0\quad 0]x(k)+v(k). \tag{32}$$

The process noise $w(k)$ is Gaussian with the zero mean value and the covariance matrix

$$W=\begin{bmatrix}0.001 & 0 & 0 & 0\\ 0 & 0.001 & 0 & 0\\ 0 & 0 & 0.001 & 0\\ 0 & 0 & 0 & 0.001\end{bmatrix}. \tag{33}$$

The measurement noise $\nu(k)$ has non-Gaussian distribution defined by (17):

$$P_\varepsilon=\{p(\nu):p(\nu)=(1-0.1)\cdot N(0;0.1)+0.1\cdot N(0;10)\}. \tag{34}$$

The transformation $T(k)$ will be determined in the algorithm (26)–(28). Taking into account the relations (17), (24), (25) and [21] for the matrix of the transformation $T(k)$, the following relation holds:

$$T^2(k)\big[H(k)P(k|k-1)H^T(k)+\sigma_N^2\big]=1. \tag{35}$$

Where from it follows that

$$T(k)=\big[H(k)P(k|k-1)H^T(k)+\sigma_N^2\big]^{-1/2}. \tag{36}$$

That value of transformation is introduced in the relations (26)–(28), which results in obtaining

$$\begin{aligned}\hat{x}(k|k)=&F(k-1)\hat{x}(k-1|k-1)+P(k|k-1)H^T(k)\\ &\times\big[H(k)P(k|k-1)H^T(k)+\sigma_N^2\big]^{-1/2}\\ &\times\psi\left(\frac{y(k)-H(k)F(k-1)\hat{x}(k-1|k-1)}{[H(k)P(k|k-1)H^T(k)+\sigma_N^2]^{1/2}}\right)\end{aligned} \tag{37}$$

$$\begin{aligned}P(k|k-1)=&F(k-1)P(k-1|k-1)F^T(k-1)\\ &+W(k-1)\end{aligned} \tag{38}$$

$$\begin{aligned}&P(k|k)\\ &=P(k|k-1)-\frac{P(k|k-1)H^T(k)H(k)P(k|k-1)}{H(k)P(k|k-1)H^T(k)+\sigma_N^2}\\ &\quad\times E_{P_\varepsilon}\left\{\psi'\left(\frac{y(k)-H(k)F(k-1)\hat{x}(k-1|k-1)}{[H(k)P(k|k-1)H^T(k)+\sigma_N^2]^{1/2}}\right)\right\}\end{aligned} \tag{39}$$

The remaining step is to determine the value $E_{P_\varepsilon}\{\psi'(\cdot)\}$. In accordance with [21], it is obtained that

$$\begin{aligned}E_{P_\varepsilon}\{\psi'(\cdot)\}&=(1-\varepsilon)[\Phi(k)-\Phi(-k)]\\ &=(1-\varepsilon)\big[2\Phi(k)-1\big],\quad 1\le k\le 3\end{aligned} \tag{40}$$

The value $\Phi(k)$ is the function of standard normal distribution

$$\Phi(k)=\frac{1}{\sqrt{2\pi}}\int_0^k e^{-\frac{x^2}{2}}dx. \tag{41}$$

The relations (37)–(41) define the robust filter for the case when the transformation $T(k)$ is used. It is seen that this

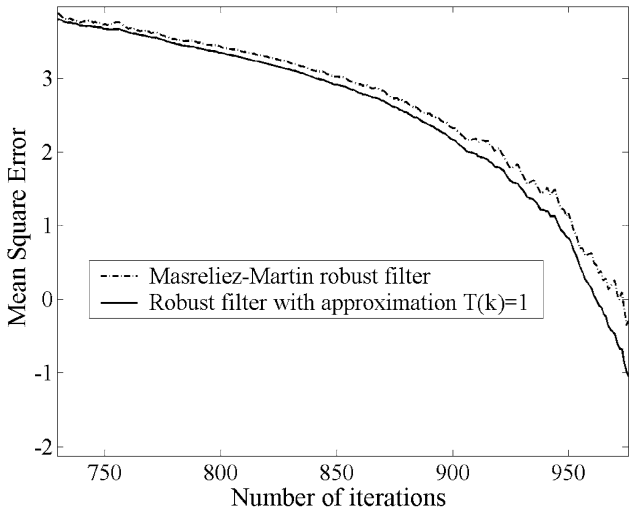

Fig. 3 Mean square error, obtained in nongaussian noise environment with contamination $\varepsilon = 0.1$

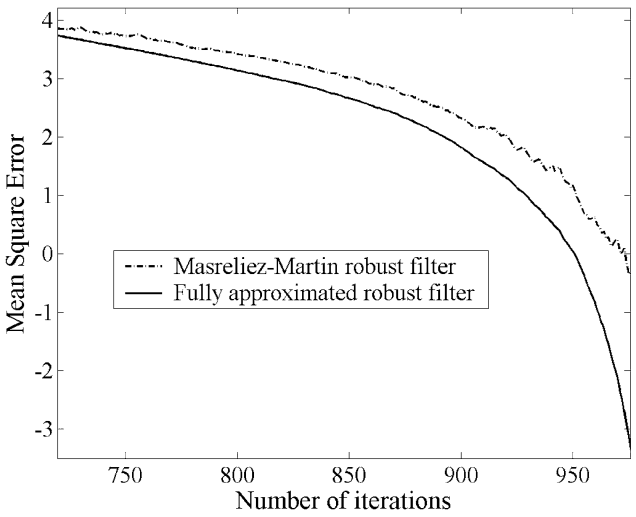

Fig. 4 Mean square error, obtained in nongaussian noise environment with contamination $\varepsilon = 0.1$

transformation complicates the relations for the filter. If the value $y(k)$ is a vector, determination of the transformation $T(k)$ requires a non-trivial numerical procedure. That is why the heuristic approximation $T(k) = 1$ is introduced in the paper ($T(k) = I$ for the case of a multivariable system).

In this case, the robust filter has the form:

$$\hat{x}(k|k) = F(k-1)\hat{x}(k-1|k-1) + P(k|k-1)H^T(k) \times \psi\big(y(k) - H(k)F(k-1)\hat{x}(k-1|k-1)\big) \quad (42)$$

$$P(k|k-1) = F(k-1)P(k-1|k-1)F^T(k-1) + W(k-1) \quad (43)$$

$$P(k|k) = P(k|k-1) - P(k|k-1)H^T(k)H(k)P(k|k-1) \times E_{P_\varepsilon}\{\psi'\big(y(k) - H(k)F(k-1)\hat{x}(k-1|k-1)\big)\} \quad (44)$$

$$E_{P_\varepsilon}\{\psi'\big(y(k) - H(k)F(k-1)\hat{x}(k-1|k-1)\big)\} = (1-\varepsilon)[2\Phi(k) - 1], \quad 1 \le k \le 3 \quad (45)$$

The value $\Phi(k)$ is determined by the relation (41).

The algorithms (37)–(41) and (42)–(45) are compared in simulations.

The following approximation is

$$E_{P_\varepsilon}\{\psi'(\cdot)\} \cong \psi'(\cdot). \quad (46)$$

The Huber's function is considered in this paper. Now the algorithm of robust filtration (with the introduced approximation $T(k) = 1$) has the form

$$\hat{x}(k|k) = F(k-1)\hat{x}(k-1|k-1) + P(k|k-1)H^T(k) \times \psi\big(y(k) - H(k)F(k-1)\hat{x}(k-1|k-1)\big) \quad (47)$$

$$P(k|k-1) = F(k-1)P(k-1|k-1)F^T(k-1) + W(k-1) \quad (48)$$

$$P(k|k) = P(k|k-1) - P(k|k-1)H^T(k)H(k)P(k|k-1) \times \psi'\big(y(k) - H(k)F(k-1)\hat{x}(k-1|k-1)\big) \quad (49)$$

The algorithm (47)–(49) represents a significantly simplified applicability of robust filters in practice. Simulation in this part of the paper represents comparison of the filters (37)–(41) and (47)–(49).

Intense simulations justified such interventions. Now the algorithm (26)–(28) obtains the modified form (47)–(49).

It is important to notice that the second heuristic modification increases the rate of convergence (47)–(49) in the initial iterations. Namely, the relations (47)–(49) for the robust Kalman filter gain result in:

$$K(k) = F(k-1)[P(k-1|k-2) - P(k-1|k-2) \times H^T(k)H(k)P(k-1|k-2) \times \psi'(\nu(k))]F^T(k-1)H^T(k) + W(k-1)H^T(k) \quad (50)$$

If

$$|\nu(k)| > k_\varepsilon, \quad \nu(k) = y(k) - H(k)F(k-1)\hat{x}(k-1|k-1) \quad (51)$$

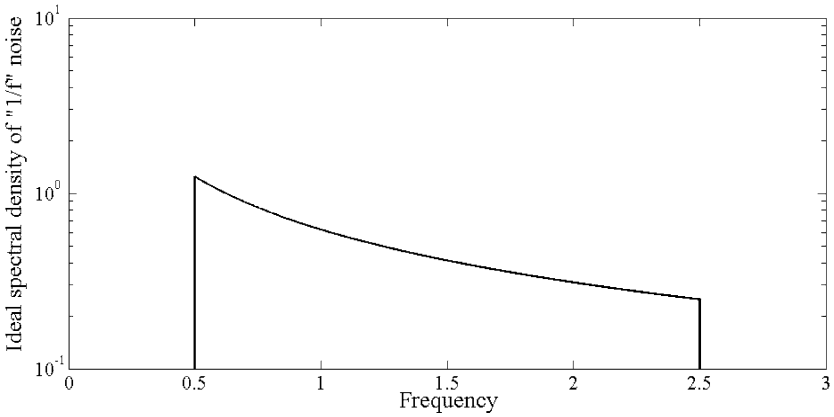

Fig. 5 Power spectral density of bandlimited '$1/f$' noise signal for $\underline{\omega} = 0.5$ and $\bar{\omega} = 2.5$

the relation (50) becomes

$$K(k) = F(k-1)P(k-1|k-2)F^T(k-1)H^T(k-1) + W(k-1)H^T(k) \tag{52}$$

because $\psi'(\nu(k)) = 0$ with the condition (51) (see Fig. 2).

By comparing the relations (50) and (52), it is seen that the gain $K(k)$ in the second case is higher. It means that the bigger the estimation errors, the higher the filter gain and thus the higher rate of estimation convergence.

By comparing the relations (8) and (14) with the relations (24) and (25) and taking care that the vector $\varphi_0(k)$ should be replaced with $\varphi(k)$ and by substituting for the values

$$F(k) = I, \qquad H(k) = \varphi^T(k), \qquad \hat{x}(k|k) = \hat{\theta}(k) \tag{53}$$

a recursive algorithm for estimation of time variant parameters is obtained in the relation (47)–(49). For transparency, the algorithm shall be given in the form of Table 1.

Table 1 Algorithm for robust identification of the system with time variant parameters

Model of change of parameters

$\theta(k+1) = \theta(k) + w(k)$

Model of measurement

$y(k) = \theta^T(k)\varphi_0(k) + \nu(k)$

A priori data

$w(k) \sim \mathrm{N}(0, W(k))$

$\nu(k) \sim (1-\varepsilon)N(0, \sigma_{N1}^2) + \varepsilon N(0, \sigma_{N2}^2), \sigma_{N2}^2 \gg \sigma_{N1}^2$

$\theta(0) \sim N(\bar{\theta}, \Sigma_\theta)$

$\mathrm{cov}\big(w(j), \nu(k)\big) = \mathrm{cov}\big(\theta(0), w(k)\big) = \mathrm{cov}\big(\theta(0), \nu(k)\big) = 0$

Replacement in the robust Kalman filter (47)–(49)

$F(k) = I, H(k) = \varphi^T(k), \hat{x}(k|k) = \hat{\theta}(k)$

Estimation of parameters

$\hat{\theta}(k) = \hat{\theta}(k-1) + P(k|k-1)\varphi(k) \cdot \psi[y(k) - \varphi^T(k)\hat{\theta}(k-1)]$

Gain coefficient

$K(k) = P(k|k-1)\varphi(k)$

A priori covariance matrix

$P(k|k-1) = P(k-1|k-1) + W(k-1)$

A posteriori covariance matrix

$P(k|k) = P(k|k-1) - P(k|k-1)\varphi(k)\varphi^T(k)P(k|k-1) \times \psi'(y(k) - \varphi^T(k)\hat{\theta}(k-1))$

Initial conditions

$\hat{\theta}(0|0) = \hat{\theta}(0) = \bar{\theta}, P(0|0) = \Sigma_\theta$

3.2 Generation of the input signal

Optimal test signals are frequently specified in terms of their second order properties, e.g. autocovariance or spectrum. This leads to the problem of implementing a real signal with specified second order properties. In addition, it is usual that the input should also be constrained in its amplitude; therefore, the amplitude must lie in an interval.

Within the constraints of its amplitude, it is important to implement an input signal which has maximum power. It is of great importance in experiment design, where the quality of estimation typically increases with the signal to noise ratio. If an input with higher power is chosen, it is obvious that the signal to noise ratio is improved. Binary signals have precisely this desirable property: their power is maximum for the given amplitude constraint.

As it is mentioned in the introductory section, the ideas from model predictive control are used to generate a binary waveform whose sampled autocovariance is as close as possible to some prescribed autocovariance [23]. Heuristically speaking, the idea is to solve, for each time instant, a finite horizon optimisation problem to find the optimal set of the next, say, T values of the sequence so that the sampled autocovariance sequence thus obtained is as close as possible (in a prescribed sense) to the desired autocovariance. One then takes the first term of this optimal set for the sequence, advances time by one step and repeats the procedure. The

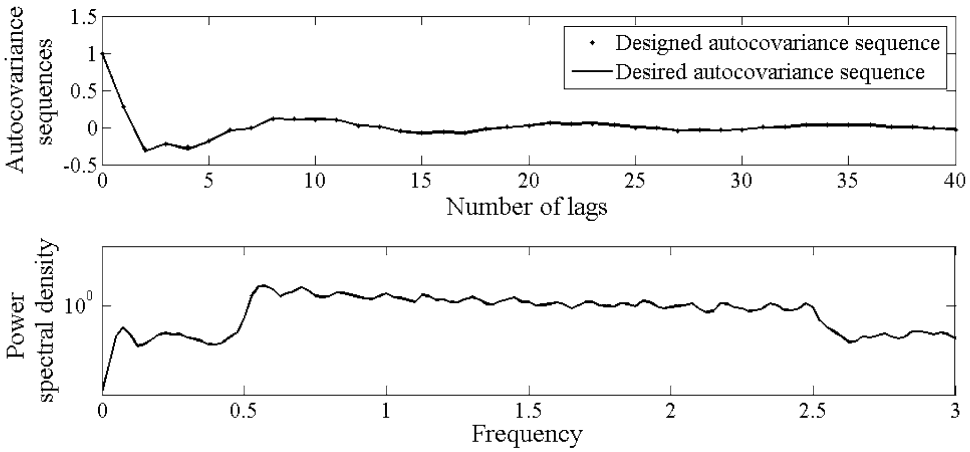

Fig. 6 Characteristics of the generated pseudo bandlimited '$1/f$' noise signal for $m = 1$, $N = 10^4$ and $n = 40$

idea behind this procedure is thus closely related to finite alphabet receding horizon control, where receding horizon concepts are employed to control a linear plant whose input is restricted to belong to a finite set.

Before the algorithm begins, the user of the algorithm has to convert the desired autocovariance sequence $\{r_k^d\}_{k=0}^{\infty}$ into the non-central autocovariance of a {0,1} sequence $\{\hat{r}_k^d\}_{k=0}^{\infty}$. Also, the user must choose three variables: N—the length of the signal to be generated, n—the number of lags $\{r_k^d\}_{k=0}^{\infty}$ to be compared to the corresponding lags of the sampled autocovariance sequence of the designed signal, and m represents the length of the receding horizon over which the optimisation algorithm is applied. For details see [23]. An outline of the algorithm is now presented as a series of steps:

1. Set $t = 1$
2. Set $(\hat{s}_t, \ldots, \hat{s}_{t+m-1}) = O_{1,m}$ where $O_{1,m}$ denotes a zero matrix of $1 \times m$ order
3. Compute the first n lags of the sampled non-central autocovariance of $(\tilde{s}, \ldots, \tilde{s}_{t-1}, \hat{s}_t, \hat{s}_{t+1}, \ldots, \hat{s}_{t+m-1})$ via

$$\hat{r}_k := \frac{1}{t+m-1} \sum_{i=k+1}^{t+m-1} \hat{s}_i \hat{s}_{i-k}, \quad k = 0, \ldots, n \tag{54}$$

   where $\hat{s}_i = \tilde{s}_i$ is considered for $i = 1, \ldots, t-1$
4. Generate a new m-tuple $(\hat{s}_t, \ldots, \hat{s}_{t+m+1}) \in \{0,1\}^m$ and repeat step 3 until all m-tuples have been tested
5. Let $\tilde{s}_t = \hat{s}_t$ for the m-tuple $(\hat{s}_t, \ldots, \hat{s}_{t+m-1}) \in \{0,1\}^m$ for which $\|\{\hat{r}_i\}_{i=0}^n - \{\tilde{r}_i^d\}_{i=0}^n\|_2$ is minimum
6. If $t < N$, let $t = t + 1$ and go to step 2
7. Convert the {0,1} N-tuple $(\tilde{s}_1, \tilde{s}_2, \ldots, \tilde{s}_N)$ into a $\{a, b\}$ N-tuple $(s_1, s_2, \ldots, s_N)$ via

$$s_t := (b-a)\tilde{s}_t + a, \quad t = 1, \ldots, N \tag{55}$$

Generation of the input signal is inspired by recent work on experiment design where it was shown that a bandlimited '$1/f$' noise has good properties in robust identification

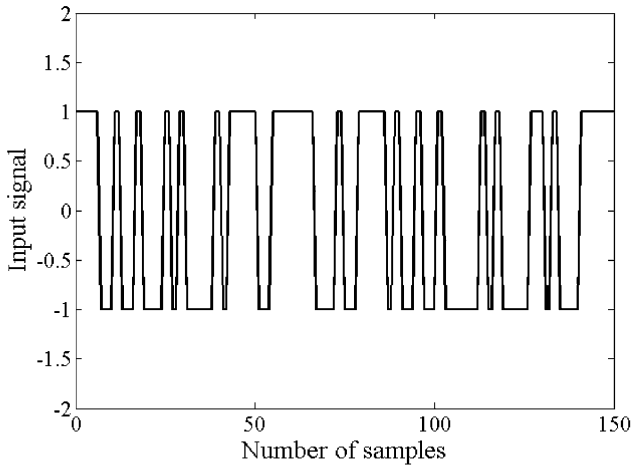

Fig. 7 Input binary sequence of generated pseudo bandlimited '$1/f$' noise signal for $m = 1$, $N = 10^4$ and $n = 40$

[24]. The bandlimited '$1/f$' noise is defined by the following spectrum:

$$\phi^{1/f}(\omega) := \begin{cases} \dfrac{1/\omega}{\ln \bar{\omega} - \underline{\omega}} & \omega \in [\underline{\omega}, \bar{\omega}] \\ 0 & \text{otherwise} \end{cases} \tag{56}$$

where $\underline{\omega}, \bar{\omega} \in R$, $(\underline{\omega} < \bar{\omega})$. The autocovariance sequence of this signal is given by

$$r_k^{1/f} := \frac{1}{\ln \bar{\omega} - \underline{\omega}} \int_{\underline{\omega}}^{\bar{\omega}} \frac{\cos kx}{x} dx, \quad k \in N_0 \tag{57}$$

Figure 5 shows the ideal spectral density of bandlimited '$1/f$' noise signal for $\underline{\omega} = 0.5$ and $\bar{\omega} = 2.5$. Figure 6 presents the results obtained from the receding horizon algorithm for $\underline{\omega} = 0.5$, $\bar{\omega} = 2.5$, $m = 1$, $N = 10^4$ and $n = 40$. This last figure verifies the ability of the algorithm to generate a binary non-white noise signal. The discrepancies between the desired and the achieved autocovariances seem to be due to the impossibility of generating a binary signal

with a true bandlimited '$1/f$' spectrum, as the results do not appear to improve significantly by increasing m and n. For more details see [23].

4 Simulation results

It has already been noted that the change of the parameters has the form of random walk, see (8). To demonstrate the performance of the proposed robust procedure for parameters estimation, it is considered the model of pneumatic cylinder whose time varying parameter vector has expected value:

$$\bar{\theta} = [-0.9131 \quad -0.3523 \quad 0.1118 \quad 0.2318 \quad -0.0413 \quad 0.0766 \quad 0.0115 \quad 0.0647]^T.$$

In the system identification example, will be considered the case when the covariance matrix of process noise $w(k)$ has the form:

$$W(k) = \begin{bmatrix} 2\cdot 10^{-6} & 0 & 0 & 0 & 0 & 0 & 0 & 0 \\ 0 & 3\cdot 10^{-6} & 0 & 0 & 0 & 0 & 0 & 0 \\ 0 & 0 & 2.5\cdot 10^{-6} & 0 & 0 & 0 & 0 & 0 \\ 0 & 0 & 0 & 2.2\cdot 10^{-6} & 0 & 0 & 0 & 0 \\ 0 & 0 & 0 & 0 & 2\cdot 10^{-8} & 0 & 0 & 0 \\ 0 & 0 & 0 & 0 & 0 & 2.2\cdot 10^{-8} & 0 & 0 \\ 0 & 0 & 0 & 0 & 0 & 0 & 2.5\cdot 10^{-8} & 0 \\ 0 & 0 & 0 & 0 & 0 & 0 & 0 & 3\cdot 10^{-8} \end{bmatrix}$$

Such models of pneumatic cylinders can be meet in exploitation with varying outdoor conditions, for example in the buses, nail guns, etc. The excitation signal was binary sequence obtained from the receding horizon algorithm.

The system identification example, is based on measured input-output data obtained during the simulations. During the simulations, it is assumed that measured noise has non-Gaussian distribution, see (17):

$$v(k) \sim (1-\varepsilon)N(0, 0.1) + \varepsilon N(0, 10).$$

From the process 1000 input-output data points were collected and loaded into MATLAB form. Figures 8 to 11 shows system output, parameter estimates, and mean square error in the case when the contamination $\varepsilon = 0.05$.

The simulation results are compared in terms of mean square error (*MSE*), defined by

$$MSE = \log\left(\left\|\hat{\theta}(k) - \theta(k)\right\|^2\right)$$

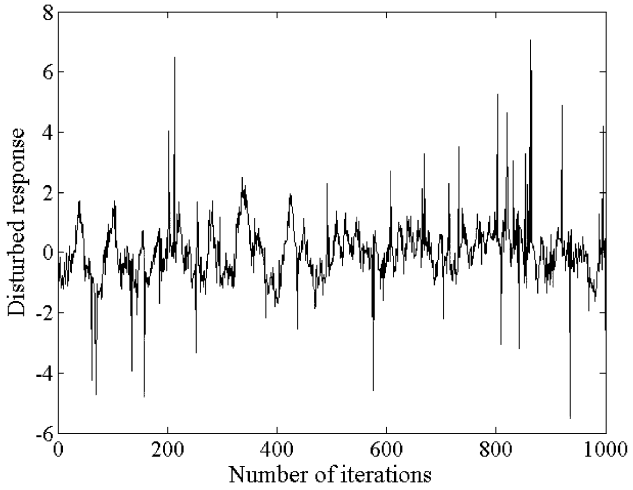

Fig. 8 Simulation of the measured output signal of the system with contamination $\varepsilon = 0.05$

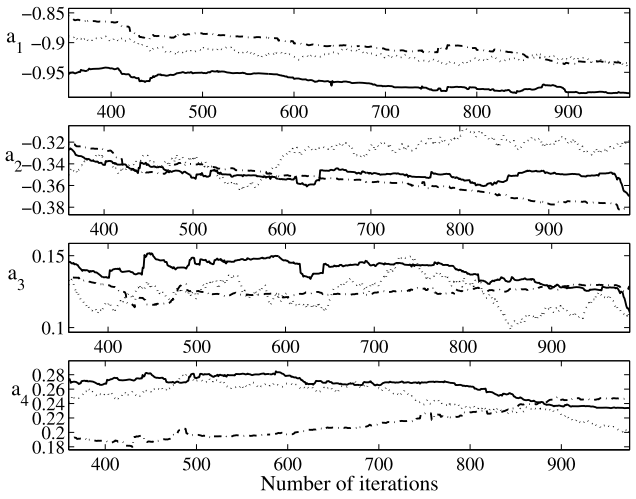

Fig. 9 Estimates of parameter a_i $(i = \overline{1,4})$, obtained in nongaussian noise environment with contamination $\varepsilon = 0.05$ (*solid line*: Robust filter, *dash-dot*: Kalman filter, *dotted line*: True time-variant parameters)

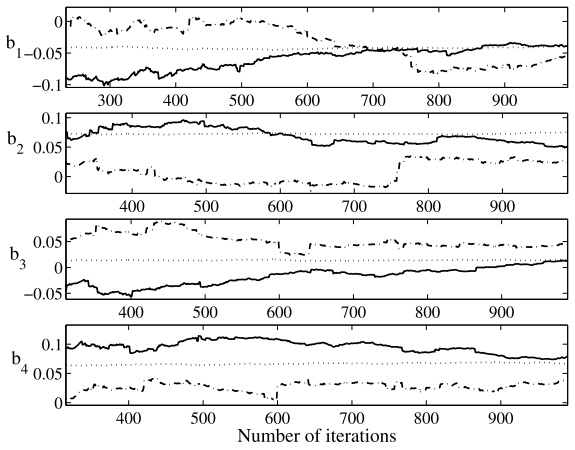

Fig. 10 Estimates of parameter b_i ($i = \overline{1,4}$) obtained in nongaussian noise environment with contamination $\varepsilon = 0.05$ (*solid line*: Robust filter, *dash-dot*: Kalman filter, *dotted line*: True time-variant parameters)

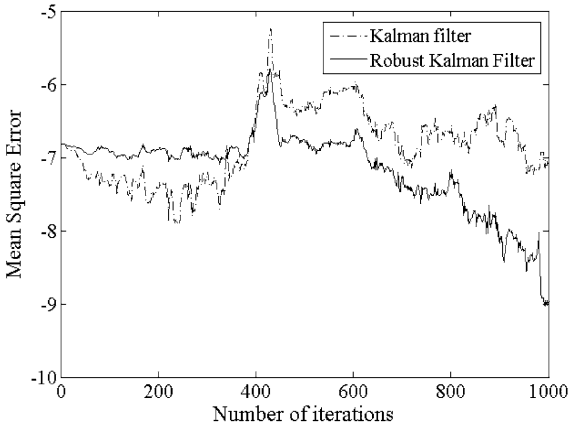

Fig. 11 Mean square error, obtained in nongaussian noise environment with contamination $\varepsilon = 0.05$

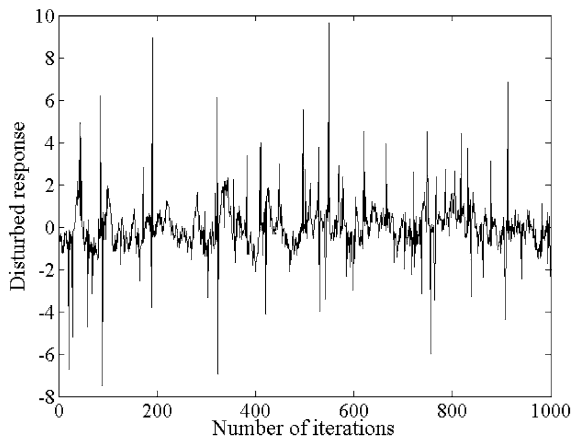

Fig. 12 Simulation of the measured output signal of the system with contamination $\varepsilon = 0.1$

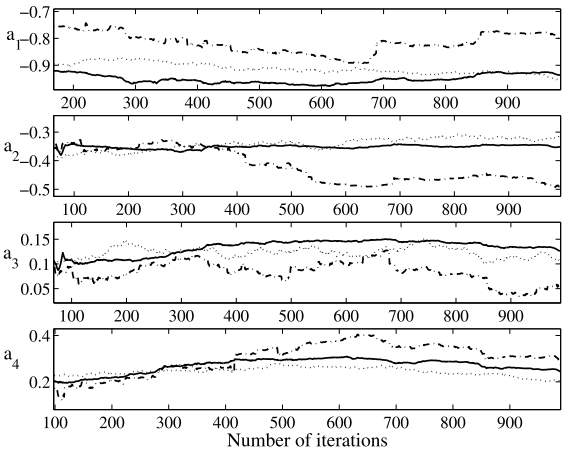

Fig. 13 Estimates of parameter a_i ($i = \overline{1,4}$) obtained in nongaussian noise environment with contamination $\varepsilon = 0.1$ (*solid line*: Robust filter, *dash-dot*: Kalman filter, *dotted line*: True time-variant parameters)

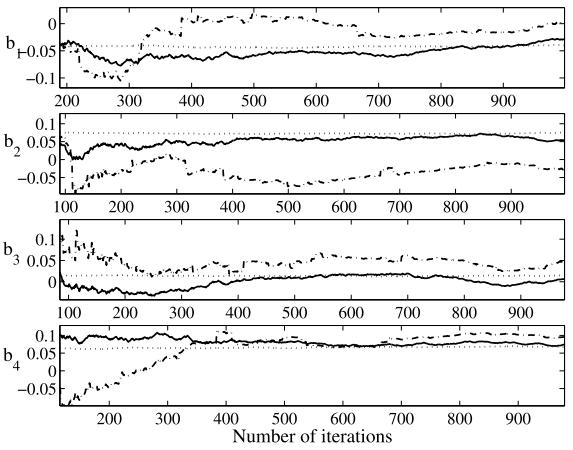

Fig. 14 Estimates of parameter b_i ($i = \overline{1,4}$) obtained in nongaussian noise environment with contamination $\varepsilon = 0.1$ (*solid line*: Robust filter, *dash-dot*: Kalman filter, *dotted line*: True time-variant parameters)

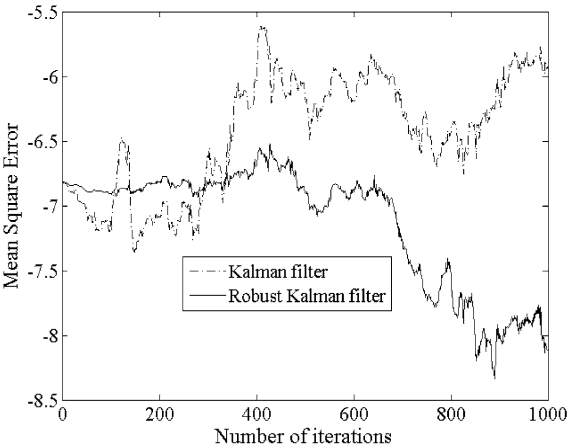

Fig. 15 Mean square error, obtained in nongaussian noise environment with contamination $\varepsilon = 0.1$

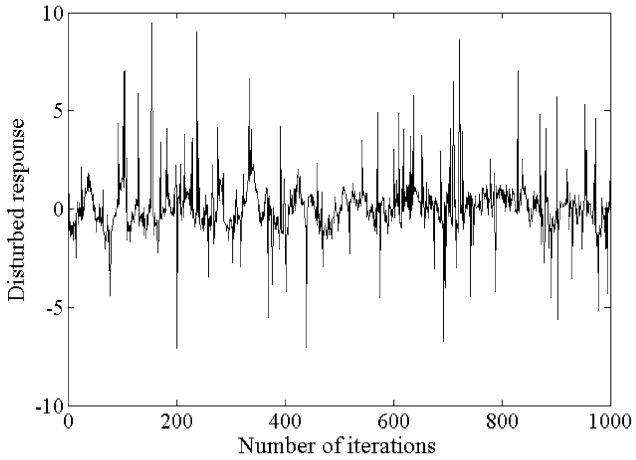

Fig. 16 Simulation of the measured output signal of the system with contamination $\varepsilon = 0.15$

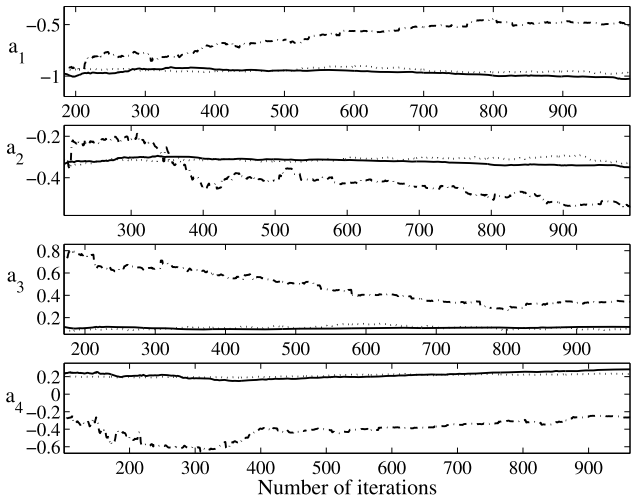

Fig. 17 Estimates of parameter a_i $(i = \overline{1,4})$ obtained in nongaussian noise environment with contamination $\varepsilon = 0.15$ (*solid line*: Robust filter, *dash-dot*: Kalman filter, *dotted line*: True time-variant parameters)

Remark 3 The presented results have shown that the classical Kalman filter is very sensitive to the nongaussian measurement noise presence, as opposed to the proposed robust Kalman filter. The proposed robust Kalman filter gives similar performance to the commonly used Kalman filter in the case of stationary pure Gaussian additive noise.

Figures 12 to 15 show system output, parameter estimates, and mean square error in the case when the contamination $\varepsilon = 0.1$.

Figures 16 to 19 show system output, parameter estimates, and mean square error in the case when the contamination $\varepsilon = 0.15$.

Comparing Figs. 11, 15 and 19, it can be clearly seen that the superiority of the modified robust Kalman filter is greater in higher degrees of contamination.

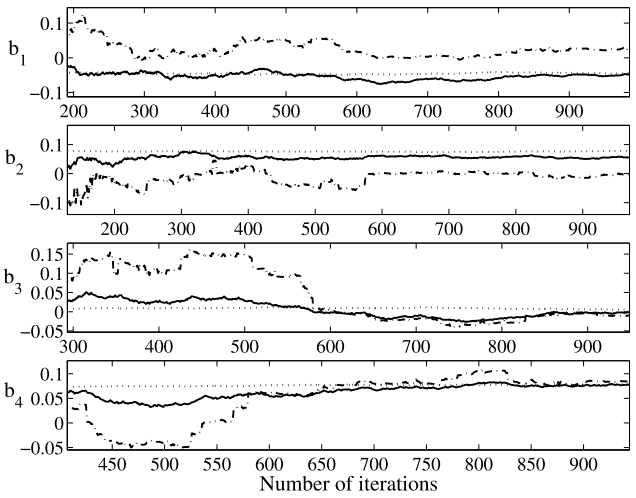

Fig. 18 Estimates of parameter b_i $(i = \overline{1,4})$ obtained in nongaussian noise environment with contamination $\varepsilon = 0.15$ (*solid line*: Robust filter, *dash-dot*: Kalman filter, *dotted line*: True time-variant parameters)

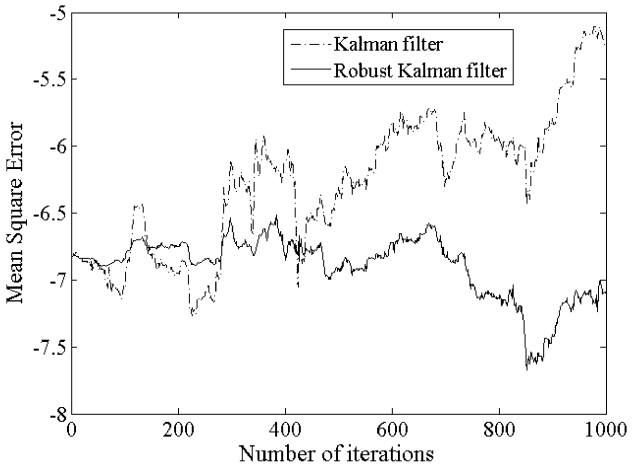

Fig. 19 Mean square error, obtained in nongaussian noise environment with contamination $\varepsilon = 0.15$

5 Conclusion

The paper considers a new mathematical model of the pneumatic cylinder. Change of parameters of the model is described by random walk. It is assumed that the cylinder is described by means of the output error model, where the measurement noise is non-Gaussian. Since the system is described with a stochastic model with variable parameters, the natural frame for identification is the Masreliez-Martin filter (the robust Kalman filter). Heuristic modifications of the mentioned filter which considerably increase its practical values were performed. Experiment design was used in identification for synthesis of input signals.

The results of this paper can be the starting point for design of an adaptive regulator. It is also necessary to create a methodology of experiment design for the case of identifica-

tion of a system with time-variant parameters (research on these problems is at its beginnings). The mentioned topics are the authors' subject of interest.

References

1. Pu J, Moore PR, Wong CB (2000) Smart components-based servo pneumatic actuation systems. Microprocess Microsyst 24:113–119
2. Shearer JJ (1956) The study of pneumatic process in the continuous control of motion with compressed air. ASME Trans 233–242
3. Anderson BW (2001) The Analysis and Design of Pneumatic System. Krieger, Melbourne
4. Wang J, Wang DJD, Moore PR, Pu J (2001) Modelling study, analysis and robust servo control of pneumatic cylinder actuator systems. IEE Proc, Control Theory Appl 148:35–42
5. Wang J, Pu J, Moore P (1999) A practical control strategy for servo-pneumatic actuator systems. Control Eng Pract 7(12):1483–1488
6. Wang J, Pu J, Moore P (1999) Accurate position control of servo pneumatic actuator systems: an application to food packaging. Control Eng Pract 7(6):699–706
7. Richard E, Scavarda S (1996) Comparison between linear and nonlinear control of an electropneumatic servodrive. J Dyn Syst Meas Control 118(2):445–452. doi:10.1115/1.2802310
8. Keller H, Isermann R (1993) Model-based nonlinear adaptive control of a pneumatic actuator. Control Eng Pract 1(3):505–511
9. Östring M, Gunnarson S, Norrlöf M (2003) Closed-loop identification of an industrial robot containing flexibilities. Control Eng Pract 11(3):291–300
10. Johansson R, Robertsson A, Nilsson K, Verhaegen M (2000) State-space system identification of robot manipulator dynamics. Mechatronics 10(3):403–418
11. AR Fraser, Daniel RW (1991) Perturbation Techniques for Flexible Manipulators. Kluwer Academic, Boston
12. Canudas C, Siciliano B, Bastin G (1996) Theory of Robot Control. Springer, New York
13. Tutunji T, Molhem M, Turki E (2007) Mechatronic systems identification using an impulse response recursive algorithm. Simul Model Pract Theory 15(8):970–988
14. Shih MC, Tseng S (1995) Identification and position control of a servo pneumatic cylinder. Control Eng Pract 3(9): 1285–1290
15. Khayati K, Bigras P, Dessaint LA (2008) Force control loop affected by bounded uncertainties and unbounded inputs for pneumatic actuator systems. J Dyn Syst Meas Control 130(1):1–9
16. Rodriguez MT, Banks SP (2010) Linear, time-varying approximations to nonlinear dynamical systems: with applications in control and optimization. Springer, Berlin
17. Barnet V, Lewis T (1994) Outliers in statistical data, 3rd edn. Wiley-Blackwell, New York
18. Huber PJ (1981) Robust statistics. Wiley, New York
19. Blackburn JF, Reethof G, Shearer JL (1960) Fluid power control. The Technology Press/Wiley, New York
20. Landau ID, Lozano R, M'Saad M (1998) Adaptive control, 1st edn. Springer, Berlin
21. Masreliez CJ, Martin RD (1977) Robust Bayesian estimation for the linear model and robustifying the Kalman filter. IEEE Trans Autom Control 22(3):361–371
22. Filipovic VZ, Kovacevic BD (1994) On robust AML identification algorithms. Automatica 30(11):1775–1778
23. Rojas R, Welsh J, Goodwin G (2007) A receding horizon algorithm to generate binary signals with a prescribed autocovariance. In: American control conference, pp. 122–127
24. Rojas R, Goodwin G, Welsh JS, Feuer A (2007) Robust optimal experiment design for system identification. Automatica 43:993–1008